TRENDS IN SCIENCES 2025; 22(7): 10441
https://doi.org/10.48048/tis.2025.10441
RESEARCH ARTICLE

Transparent P(VDF-HFP) Coatings for Enhancing Fungal Resistance, Hydrophobicity, and Durability of Krajood-Based Natural Fibers

Sirikun Pethuan[1], Nattavadee Tammachat[1], Chaiporn Kaew-on[1], Ratchaneewan Siri[2], Nikruesong Tohluebaji[3], Phongpichit Channuie[4] and Jureeporn Yuennan[1,*]

[1]*Faculty of Science and Technology, Nakhon Si Thammarat Rajabhat University, Nakhon Si Thammarat 80280, Thailand*
[2]*Division of Physical Science (Physics), Faculty of Science, Prince of Songkla University, Songkhla 90112, Thailand*
[3]*Faculty of Science and Technology, Princess of Naradhiwas University, Narathiwat 96000, Thailand*
[4]*School of Science, Walailak University, Nakhon Si Thammarat 80160, Thailand*

([*]Corresponding author's e-mail: jureeporn_yue@nstru.ac.th)

Received: 22 April 2025, Revised: 5 June 2025, Accepted: 10 June 2025, Published: 15 June 2025

ABSTRACT

This study investigates the use of poly(vinylidene fluoride-co-hexafluoropropylene) [P(VDF-HFP)] as a transparent, water-repellent, and antifungal coating for Krajood (*Lepironia articulata*) products—traditional natural fibers widely used in Thailand. Coatings with P(VDF-HFP) were formulated at concentrations ranging from 2.5 to 25% and applied via a solution casting technique. The surface, thermal, mechanical, and biological properties of the coated samples were systematically characterized and compared to uncoated and lacquer-coated controls using Fourier-transform infrared spectroscopy (FTIR), water contact angle (WCA) measurements, thermogravimetric analysis (TGA), scanning electron microscopy (SEM), and tensile testing. Results indicate that the 15% P(VDF-HFP) coating provides the most optimal performance, offering high hydrophobicity (WCA = 124.2°), enhanced tensile strength (112.26 MPa), superior thermal resistance (onset degradation at 241.9 °C), and significant fungal inactivation over a 30-day incubation period. The formation of a microporous surface structure, due to slow solvent evaporation, was found to play a key role in improving both water repellency and fungal resistance. These findings demonstrate the potential of P(VDF-HFP) coatings in extending the lifespan and functionality of natural fiber products, providing a sustainable alternative for moisture-prone applications.

Keywords: Hydrophobicity, Antifungal coating, P(VDF-HFP), Water-repellent coating, Natural fibers

Introduction

Natural fibers have gained increasing attention as eco-friendly and biodegradable alternatives to synthetic materials in the development of sustainable products. Among these, *Krajood* (*Lepironia articulata*), a wetland sedge native to Southeast Asia, is traditionally used in rural Thailand for weaving mats, bags, and home décor due to its strength, flexibility, and cultural significance [1]. However, like other lignocellulosic fibers, Krajood is highly hydrophilic and prone to degradation in humid environments. Moisture absorption promotes microbial colonization—particularly fungi—leading to discoloration, odor, and a significant reduction in mechanical integrity, thereby limiting the shelf life and broader applicability of Krajood-based products [2]. Conventional surface treatments, such as the application of natural lacquer, have been employed to improve water resistance and visual appeal. However, lacquer coatings often form brittle films that crack over time and offer only modest improvements in hydrophobicity and antifungal resistance [3-5]. Additionally, the need for non-toxic, transparent, and flexible coatings has prompted research into advanced polymer-based

protective layers that can offer multifunctional performance without altering the natural aesthetics of the fiber.

In this context, fluorinated polymers—particularly poly(vinylidene fluoride-co-hexafluoropropylene) [P(VDF-HFP)]—have demonstrated outstanding potential due to their unique physicochemical properties [6]. This copolymer integrates the rigidity of vinylidene fluoride (VDF) with the flexibility of hexafluoropropylene (HFP), forming a semi-crystalline structure characterized by excellent thermal and chemical resistance, low surface energy, and high optical transparency [7,8]. The exceptional thermal and chemical resistance of P(VDF-HFP) is attributed to its molecular architecture: the vinylidene fluoride units form a semi-crystalline backbone that provides thermal stability, while the hexafluoropropylene units introduce flexibility and disrupt crystallinity. The strong carbon–fluorine (C–F) bonds present in both monomers are highly stable and chemically inert, allowing the copolymer to resist degradation from heat, oxidation, and exposure to a wide range of chemicals [9]. These attributes make P(VDF-HFP) highly suitable for applications in membrane technology, biomedical devices, and protective surface coatings. The intrinsic hydrophobicity of P(VDF-HFP) stems from its fluorinated molecular architecture, which minimizes surface polarity, thereby resisting wetting and biological contamination such as biofouling. Moreover, when P(VDF-HFP)-based coatings are processed through slow solvent evaporation, microporous surface morphologies may emerge, enhancing surface roughness and amplifying water repellency through the Cassie-Baxter effect—thereby promoting self-cleaning and antifungal functionality [10-12]. Notable advancements in the use of P(VDF-HFP) include the work of Spasova *et al.* [13], who developed superhydrophobic nanofibrous mats combining PVDF and P(VDF-HFP) with ZnO nanoparticles and the antimicrobial agent 5-chloro-8-hydroxyquinolinol (5Cl8HQ). These mats displayed superior water repellency, thermal stability, and antibacterial performance. Likewise, Zhang *et al.* [14] fabricated porous P(VDF-HFP)/PVDF films with hierarchical micro/nanostructures that facilitated radiative cooling (achieving a 16 °C sub-ambient temperature drop) along with robust self-cleaning capability, proving their multifunctional potential for long-term use. Additionally, Tournis *et al.* [15] reported on the surface modification of porous P(VDF–HFP) membranes with fluorinated silicon nanoparticles, significantly increasing the water contact angle from 124 ± 2 to $174 \pm 3°$, and thereby improving hydrophobicity, fouling resistance, and membrane permeability for water treatment applications. Despite its extensive application in filtration and electronic devices, the use of P(VDF-HFP) as a water-repellent protective coating for natural fibers such as Krajood remains largely unexplored. Notably, Žigon *et al.* [16] recently introduced a novel multifunctional coating for wood based on P(VDF-HFP), polyvinylpyrrolidone (PVP), and molybdenum trioxide (MoO_3) nanowires. This formulation exhibited excellent adhesion to beech wood, producing elastic films up to 40 µm thick. The coating significantly improved hydrophobicity—elevating the water contact angle from 46° to 123°—while also providing resistance to water, alcohol, and dry heat. The presence of MoO_3 contributed antimicrobial activity, effectively suppressing blue-stain fungi and mold development. Taken together, these findings highlight the multifunctionality of P(VDF-HFP)-based coatings and underscore the need for systematic investigations into their performance on natural lignocellulosic substrates. Therefore, exploring the effects of various P(VDF-HFP) concentrations on the surface, thermal, and antifungal properties of Krajood is essential for optimizing its application as a sustainable, protective biocoating. A preliminary version of this research was previously published in Thai language [17]. In the present study, however, all experimental procedures were repeated with newly prepared samples, and all results reported herein are newly generated. The scope of this work is significantly broader, with detailed analyses and improved characterization protocols that were not included in the prior publication.

This study aims to evaluate the effectiveness of P(VDF-HFP) as a multifunctional coating for Krajood sheets by preparing solutions with various polymer concentrations (2.5 - 25%) and applying them via a simple casting method. Uncoated and lacquer-coated samples were used as controls. The coated samples were characterized through a suite of analytical techniques, including Fourier-transform infrared spectroscopy

(FTIR), thermogravimetric analysis (TGA), differential thermal analysis (DTA), water contact angle (WCA) measurement, scanning electron microscopy (SEM), and tensile strength testing. Additionally, fungal cultivation assays were conducted to evaluate the biological resistance of the coatings over 30 days. By correlating microstructural features with functional properties, this study identifies the optimal P(VDF-HFP) concentration for extending the service life and hygiene of Krajood products, contributing to the development of durable, biodegradable materials for sustainable applications.

Materials and methods

Chemicals, P(VDF-HFP) solution preparation, and coating process on Krajood samples

Poly(vinylidene fluoride-co-hexafluoropropylene) [P(VDF-HFP), Solef® 11010/1001] was used as the base polymer for the water-repellent coating. This polymer, supplied by Solvay (Bangkok, Thailand), has a melt mass-flow rate (MFR) of 4 - 8 g/10 min at 230 °C under a 5 kg load, a density of 1.78 g/cm³, a melting temperature range of 158 - 162 °C, and a water absorption rate below 0.04% at 23 °C over 24 h. All samples used in this study were freshly prepared using updated methodologies. Unlike our previous study, in which the samples were oven-dried at 60 °C, the Krajood samples in this study were air-dried at room temperature. This change aimed to preserve the fiber structure and improve coating uniformity. Each experiment was conducted under tightly controlled environmental conditions, and all measurements were performed in triplicate to ensure reproducibility and statistical accuracy. The P(VDF-HFP) powder was dissolved at concentrations of 2.5, 5, 10, 15, 20 and 25% by weight in 100 mL of N,N-Dimethylformamide (DMF, AR1051-G4L; density 0.949 g/cm³), a highly polar solvent obtained from RCI Labscan (Thailand). For each solution, the required amount of polymer was weighed and added to the solvent in a 250 mL beaker. A magnetic stir bar was placed in the beaker, which was then covered with aluminum foil to prevent contamination and solvent evaporation. While the general experimental approach was based on prior exploratory work, all sample preparations, measurements, and characterizations were repeated under controlled and standardized conditions to ensure accuracy, reproducibility, and comparability. The mixture was stirred at room temperature (30 °C) until the polymer fully dissolved, resulting in a clear, bubble-free solution. Once homogeneity was achieved, the solution was transferred to a clean glass bottle and stored at room temperature for subsequent use in coating Krajood sheets, as illustrated in **Figure 1(a)**. The prepared P(VDF-HFP) polymer solution was applied to Krajood samples using a solution casting method. The Krajood material used in this study was in its raw, untreated form and had not undergone any prior drying or surface modification. Each sample was coated 3 times, with the solution applied evenly to both sides using a brush. A total of 5 square samples, each measuring 5×5 cm^2 with a thickness of 0.5 cm, were prepared for subsequent testing. After the final coating, all samples were air-dried at room temperature until completely dry. Unlike our previous study [17], where the coated samples were oven-dried at 60 °C, in the present work, all Krajood samples were air-dried at room temperature to better preserve the natural fiber structure and surface characteristics prior to composite preparation. The coated samples were then subjected to analysis and compared with both uncoated and lacquer-coated Krajood to evaluate and compare their performance characteristics.

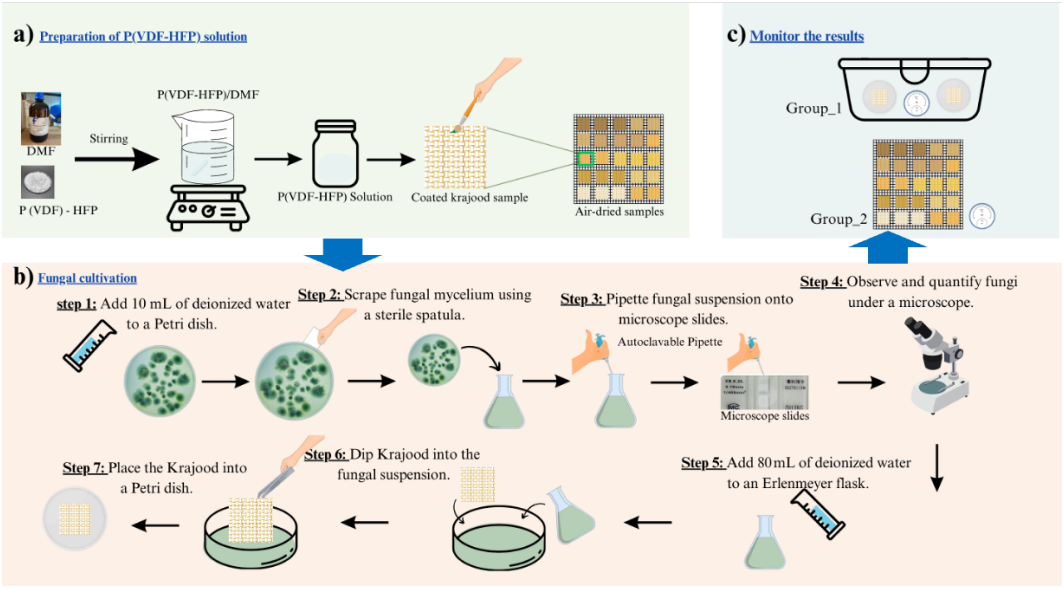

Figure 1 (a) Preparation of P(VDF-HFP) solution and coating onto Krajood samples, (b) fungal cultivation steps including suspension preparation, spore quantification, and sample inoculation and (c) storage setup for monitoring fungal growth under 2 conditions over 30 days.

Characterization of P(VDF-HFP) solution and coated Krajood products

Solution properties

Viscosity

The viscosity of the water-repellent solution was measured using a Digital Viscometer (model LV DV-I Prime, Brookfield, USA), which is renowned for its precision in directly assessing dynamic viscosity. Testing was conducted at a controlled temperature of 25.8 - 26.0 °C with a 20 mL sample volume, and the viscosity was reported in centipoise (cP) along with the standard deviation (SD) to ensure measurement accuracy. The rheometric technique was employed to evaluate the solution's flow characteristics under standardized conditions, following the WI-RES-Visco-001 method, thereby ensuring consistency and reliability in the viscosity results.

Surface tension

Surface tension reflects the force stabilizing a liquid's surface, resulting from cohesive molecular interactions. When a droplet forms at a needle's tip, it grows until the surface tension can no longer counteract gravity, providing a measurable parameter. Surface tension decreases with increasing temperature as molecular cohesion weakens [18]. In this study, the surface tension of the P(VDF-HFP) solution was evaluated at room temperature using a Dataphysics Contact Angle System (OCA-15EC, Germany) equipped with SCA20_U software in pendant drop mode. The liquid's density was measured beforehand, and 20 µL droplets were dispensed at a very slow rate to ensure accurate droplet formation. For each sample, 3 droplet images were captured just before detachment from the syringe tip, enabling precise analysis and averaging of the surface tension values. The droplet's shape was governed by the equilibrium between surface tension at the needle tip and the droplet's gravitational force, allowing the calculation of surface tension using the Young-Laplace equation [19]:

$$\gamma = \frac{\Delta\rho g D_E^2}{H}, \quad (1)$$

where γ represents the surface tension (N/m), $\Delta\rho$ is the density difference between the liquid and air, g is gravitational acceleration, D_E is the droplet's maximum diameter, and $1/H$ is the geometric correction factor. The correction factor $1/H$ is further defined as [19]:

$$\frac{1}{H} = a\left(\frac{D_S}{D_E}\right)^b, \quad (2)$$

where D_s is the droplet diameter at a specific height from the bottom, with constants a ≈ 0.345 b ≈ −2.5. These calculations ensure precise surface tension measurements by analyzing the droplet geometry.

Coated product properties

Optical transparency

The optical transparency of the coating was evaluated to determine its impact when applied to Krajood. The transparency assessment involved visual inspection and measurement techniques to observe any changes in appearance, ensuring the coated Krajood retained its natural aesthetic. This evaluation was essential to confirm that the P(VDF-HFP) coating provided water-repellent and antifungal properties without significantly altering the visual quality of the Krajood material.

Water contact angle (WCA)

The water contact angle (WCA) serves as a key indicator of surface wettability, revealing the extent of interaction between a liquid and a surface. Hydrophilic surfaces promote droplet spreading and flattening, while hydrophobic surfaces maintain a spherical droplet shape, highlighting the varying levels of adhesion between the liquid and the surface. According to Young's equation, this relationship is expressed as [20]:

$$cos\theta = (\frac{\gamma_{SG}-\gamma_{LS}}{\gamma_{LG}}). \quad (3)$$

where γ_{SG} is the surface energy between the solid and gas, γ_{LS} is the surface energy between the liquid and solid, γ_{LG} is the surface energy between the liquid and gas, and θ is the contact angle. In this study, WCA measurements were conducted using a Dataphysics Contact Angle System (OCA-15EC, Germany) equipped with SCA20_U software in sessile drop mode. Water droplets of 2 µL were dispensed onto the Krajood samples placed on a sample holder. Three droplets were applied to each sample, and images were captured to analyze the contact angles, which were then averaged. For rough surfaces, the WCA is further explained by the Cassie-Baxter equation [20]:

$$cos\theta_{CB} = f_1(cos\theta_1 + 1) - 1, \quad (4)$$

where θ_{CB} is the Cassie-Baxter contact angle, f_1 represents the fraction of the liquid-solid contact area, and θ_1 is the contact angle on a flat, smooth surface. The Cassie-Baxter model explains how liquids interact with rough surfaces by proposing that the liquid primarily contacts the peaks of the surface roughness, while air pockets are trapped in the valleys. This inclusion of air lowers the overall surface energy, resulting in larger contact angles and enhanced hydrophobicity [21]. The model provides valuable insights into how surface roughness contributes to the improved hydrophobic performance observed in the coated Krajood samples.

FTIR analysis

To identify the presence of chemical bonds on the membrane surface, Attenuated Total Reflection - Fourier Transform Infrared Spectroscopy (ATR-FTIR) was employed. This technique was utilized to investigate the interactions between the surface of Krajood coated with lacquer and PVDF-HFP polymer. FT-IR analysis was performed using an INVENIOS Bruker (Germany) instrument equipped with an attenuated total reflectance (ATR) accessory featuring a Diamond crystal. The measurements were conducted within the wavenumber range of 400 - 1000 cm^{-1}.

Thermal analysis

Thermal analysis is a branch of materials science that examines the properties of materials, such as Krajood coated with lacquer and P(VDF-HFP) polymer, as they change with temperature. Thermogravimetric analysis (TGA), derivative thermogravimetry (DTG), and differential thermal analysis (DTA) were performed using a simultaneous DTATGA thermal analyzer apparatus (Thermogravimetric Analyzer, METTLER TOLEDO, Switzerland) equipped with a platinum pan. Measurements were conducted over a temperature range of 25.0 to 600.0 °C, with a heating rate of 10.0 °C/min, under a nitrogen atmosphere at a flow rate of 20.0 mL/min.

Mechanical properties

Tensile testing was conducted on Krajood fibers, both coated (with water-repellent solution and lacquer) and uncoated, to assess their mechanical properties. Using a Zwick Roell tensile testing machine (model Z010) with a 1.0 kN load cell and a test speed of 100 mm/min, each sample was tested 5 times for accuracy and reliability. The stress-strain data generated from these tests allowed for the calculation of Young's modulus, which measures material stiffness based on Hooke's Law [22]. Stress (σ) was calculated using the

formula $\sigma=F/A$, where F is the applied force and A is the original cross-sectional area of the sample. Strain (ε) was determined by $\varepsilon=\Delta L/L_0$, with ΔL as the change in length and L_0 as the original length. Young's modulus (E) was then calculated as the ratio of stress to strain in the elastic region, given by $E=\sigma/\varepsilon$. These calculations provided insights into the material's stiffness and resistance to deformation, valuable for material improvements and process optimization in Krajood fiber applications.

Fungal inactivation testing

Krajood sheets were used as substrates for fungal cultivation. Initially, the sheets were lightly misted with water and left overnight to increase moisture content, promoting fungal growth. The moistened samples were then cut into small strips and surface-sterilized by immersion in Clorox (sodium hypochlorite) for 1 min, followed by 2 rinses with deionized water and blot drying. Sterilized samples were placed on potato dextrose agar (PDA) plates, sealed in plastic bags with rubber bands, and incubated under humid conditions for 6 days to encourage fungal colonization. As multiple fungal strains may develop on a single plate, sub-culturing was conducted to isolate pure colonies. Selected strains were transferred to fresh PDA plates, sealed with Parafilm, and incubated until pure cultures were obtained. These were then preserved in agar-containing test tubes for future use.

For fungal inoculation, as illustrated in **Figure 1(b)**, 10 mL of deionized water was added to a Petri dish containing fungal mycelium. The mycelium was scraped using a sterile microscope slide and transferred to an Erlenmeyer flask. An automatic pipette was used to place the fungal suspension onto microscope slides for spore quantification. After dilution calculations, 80 mL of deionized water was added to further dilute the spore suspension. Subsequently, 20 mL of the diluted suspension was dispensed into sterile Petri dishes, allowing immersion of up to 5 Krajood sheets per dish. The Krajood samples were immersed in the suspension using sterile forceps, ensuring both sides were thoroughly soaked, and then transferred to clean, covered Petri dishes for incubation.

As illustrated in **Figure 1(c)**, the inoculated Krajood samples were divided into 2 storage conditions: the first group was placed in a sealed plastic container, while the second was stored in a drawer within an open-air laboratory environment. Both groups were monitored over a 30-day period. Temperature and humidity were continuously recorded using a Mijia Square Temperature and Humidity Sensor (Bluetooth 4.2; Xiaomi, China) to maintain consistent environmental conditions. Visual observations were conducted by photographing the samples on days 5, 10, 15, 20, 25, and 30 to monitor the progression of fungal growth. After the 30-day incubation period, surface morphology and fungal attachment were analyzed using scanning electron microscopy (SEM). Prior to imaging, all samples were sputter-coated with a thin layer of gold to enhance surface conductivity. High-resolution imaging was performed using a Hitachi SU3900 SEM (Hitachi, Japan) at an accelerating voltage of 5 kV, providing optimal resolution while preserving the structural integrity of the Krajood surfaces. Microstructural analysis was conducted at magnifications of 500×, 1k×, 5k×, and 10k× to assess the distribution and attachment behavior of fungal colonies on samples treated with different coatings.

Results and discussion

Characterization of P(VDF-HFP) solution

Viscosity of P(VDF-HFP) Solution

The viscosity of P(VDF-HFP) solutions demonstrates a strong dependence on polymer concentration, as depicted in **Figure 2**. At lower concentrations, such as 2.5 and 5.0%, the viscosity values are 5.27 and 16.2 cP, respectively, indicating relatively low resistance to flow. This can be attributed to the reduced intermolecular interactions at lower polymer densities. As the concentration increases to 10.0 and 15.0%, the viscosity rises significantly to 72.3 and 224.9 cP, respectively. This sharp increase suggests that the polymer chains interact more extensively, forming entanglements and networks within the solvent, which impede flow. At 20.0% concentration, the viscosity spikes dramatically to 650.9 cP, reflecting a near-gel-like state of the solution. This behavior is indicative of extensive molecular entanglement and strong cohesive forces within the polymer-solvent system, which substantially hinder the movement of the solution. However, at the 25.0% concentration, viscosity could not be measured (N/A), likely due to the solution's extreme thickness or gelation, which prevents accurate

flow measurements using standard viscometry techniques. These findings highlight the critical role of concentration in determining the processing characteristics of P(VDF-HFP) coatings. Low-viscosity solutions (e.g., 2.5 - 5.0%) are ideal for achieving thin, uniform coatings, while high-viscosity solutions (10.0 - 20.0%) may provide thicker, more robust layers. However, overly high viscosities, as observed at 25.0%, can hinder coating uniformity and processability, underscoring the importance of optimizing concentration to balance application ease and coating performance. This understanding is crucial for tailoring P(VDF-HFP) solutions to specific coating requirements, ensuring both functionality and efficiency in application processes.

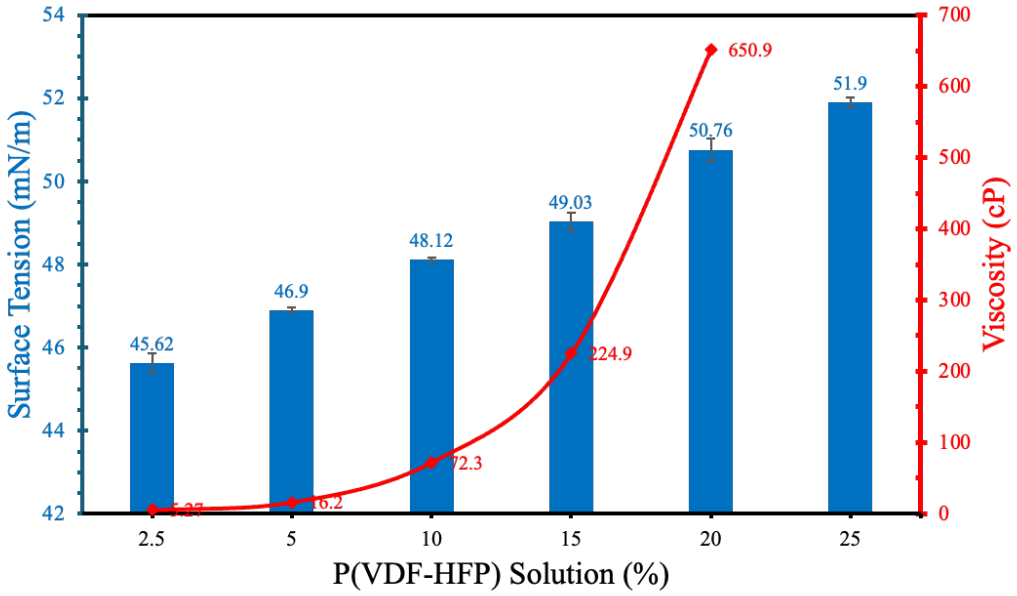

Figure 2 Surface tension and viscosity of P(VDF-HFP) solutions at various concentrations ranging from 2.5 to 25.0%.

Surface tension of P(VDF-HFP) solution

The surface tension of P(VDF-HFP) solutions increases progressively with polymer concentration, aligning with the viscosity results, as shown in **Figure 2**. At lower concentrations of 2.5 and 5%, the surface tension values are 45.62 ± 0.23 and 46.90 ± 0.06 mN/m, respectively, indicating minimal disruption of the liquid-air interface. This behavior is attributed to the lower density of polymer chains at these concentrations, resulting in less significant intermolecular forces acting at the surface. As the concentration increases to 10 and 15 %, the surface tension rises to 48.12 ± 0.05 and 49.03 ± 0.22 mN/m, respectively. This trend suggests enhanced polymer chain interactions and entanglement, which strengthen the cohesive forces within the liquid, increasing resistance to deformation at the liquid-air interface and leading to higher surface tension values. At concentrations of 20 and 25%, the surface tension reaches 50.76 ± 0.27 and 51.90 ± 0.11 mN/m, respectively. These higher values reflect significant polymer network formation near the surface, resulting in a more rigid interfacial layer. The effect is further amplified at 25.0% concentration due to the higher density of polymer chains; however, the viscosity at this level becomes too high for standard measurements. The increasing surface tension with concentration underscores the importance of achieving a critical balance when formulating P(VDF-HFP) solutions for coating Krajood surfaces. While higher surface tension may enhance coating stability and adhesion, it also poses challenges for uniform coating application due to increased viscosity. Therefore, optimizing both surface tension and viscosity is crucial to ensuring effective performance in Krajood coating applications.

Characterization of coated Krajood products

Optical transparency

Figure 3 illustrates the effects of different coatings on natural Krajood, comparing uncoated, lacquer-coated, and P(VDF-HFP) polymer-coated

samples at concentrations ranging from 2.5 to 25%. The uncoated and lacquer-coated samples retain the original texture and color of Krajood, preserving its natural aesthetic. At lower polymer concentrations (2.5 - 10%), the coatings impart a slight gloss without altering the natural appearance, making them ideal for decorative purposes. However, as the concentration increases (15 - 20%), the Krajood surface exhibits a slight reduction in transparency. At the highest concentration (25%), the polymer coatings significantly reduce transparency, displaying a white coloration that partially obscures the natural texture of the material. These results emphasize the importance of balancing visual appeal and functionality. Lower concentrations (2.5 - 10%) are better suited for decorative applications, while higher concentrations (15 - 25%) provide enhanced durability, making them more suitable for functional uses that extend the material's lifespan. Similarly, research on Polyborneolacrylate (PBA) polymer coatings on paper demonstrated strong antifungal properties [23]. These coatings worked by creating a surface structure that minimized fungal attachment without relying on toxic chemicals. The study found that a 10% concentration offered optimal antifungal protection while preserving the paper's natural qualities, such as color and strength. This example highlights the versatility of polymer coatings, including P(VDF-HFP), in effectively protecting materials while maintaining their original appearance and properties.

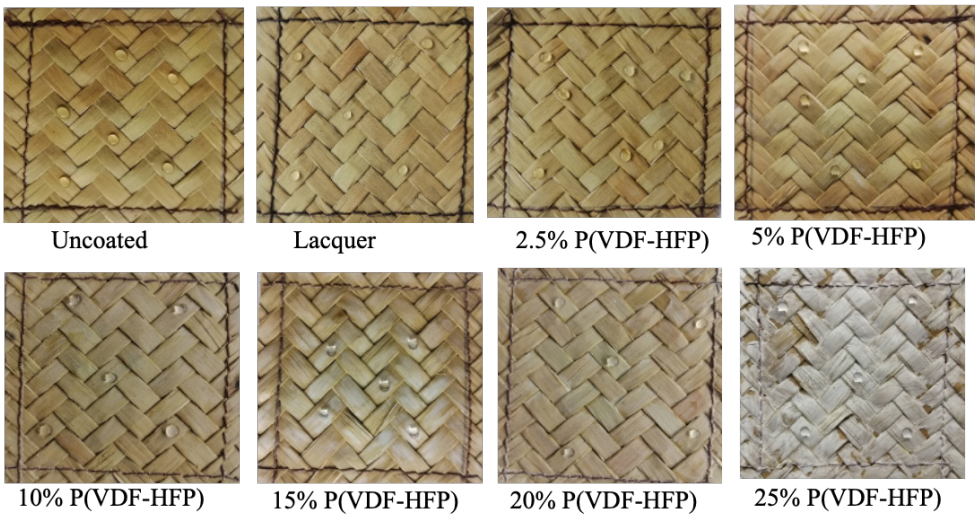

Figure 3 Digital images of water droplet behavior on the surface of Krajood products with different surface treatments: uncoated (control), lacquer-coated, and coated with P(VDF-HFP) solutions at varying concentrations of 2.5, 5, 10, 15, 20 and 25%.

Water contact angle (WCA)

The water contact angle (WCA) analysis presented in **Figure 4** illustrates the progressive increase in water repellency of Krajood products with higher concentrations of P(VDF-HFP) coating. Uncoated Krajood samples displayed moderate hydrophobicity with an average WCA of 95.81°, attributed to the natural roughness and structure of the fibers, which provide limited resistance to water. Coating with lacquer slightly improved the WCA to 99.70°, offering minimal enhancement due to its smooth, protective nature rather than significant hydrophobic properties. However, as the concentration of P(VDF-HFP) increased, the WCA rose markedly, reaching 130.93° at 25.0%, demonstrating substantial hydrophobic improvement. This transition is likely influenced by the formation of micro- and nano-scale surface textures, inspired by natural hydrophobic surfaces such as lotus leaves. According to the Cassie-Baxter model, these hierarchical structures trap air between the droplet and the solid surface, reducing the effective liquid-solid contact area. This results in lower adhesion and enhanced water repellency, as evidenced by the increase in water contact angle observed in the coated samples. This enhancement is attributed to several key factors. First, the fluorinated structure of P(VDF-HFP) provides

inherently low surface energy, significantly reducing the wetting behavior of water. Fluorinated polymers are particularly effective as their highly electronegative fluorine atoms create non-polar surfaces, minimizing water adhesion and spreading [24,25]. Second, the coating process increases surface roughness, amplifying the hydrophobic effect through the Wenzel and Cassie-Baxter models. The Wenzel model suggests that roughness enhances the material's inherent hydrophobicity by increasing the actual surface area, while the Cassie-Baxter model explains how trapped air pockets beneath water droplets reduce the solid-liquid contact area, leading to improved water repellency. Micro- and nano-scale texturing, inspired by natural hydrophobic surfaces like lotus leaves, likely contributes to this transition [26,27]. Additionally, higher concentrations of P(VDF-HFP) result in thicker and more uniform coatings, which not only reduce surface defects but also enhance durability by preventing water penetration. Uniform coatings improve the longevity of the hydrophobic effect, ensuring consistent water repellency over time [20,28]. The results confirm that P(VDF-HFP) coatings significantly enhance the hydrophobicity and durability of Krajood products, making them suitable for applications in humid or wet environments where water resistance is crucial. These findings highlight the potential of P(VDF-HFP) as an innovative material for creating highly water-repellent surfaces through a combination of low surface energy, enhanced roughness, and uniform layer formation. Notably, some differences in the values of viscosity and water contact angle compared to our earlier report were observed. These variations can be attributed to differences in ambient humidity, solvent evaporation rates, and the dispersion quality of nanoparticles during the spray-coating process. In the present study, more rigorous control of environmental conditions and procedural parameters was implemented, and all measurements were conducted in triplicate to ensure statistical reliability. Furthermore, unlike our previous work, where samples were oven-dried at 60 °C, the Krajood samples in this study were air-dried at room temperature. This modification aimed to better preserve the natural fiber structure and surface characteristics prior to fabrication. Compared to the preliminary findings, the current results exhibit improved consistency and a broader range of material performance, as confirmed by detailed SEM and FTIR analyses.

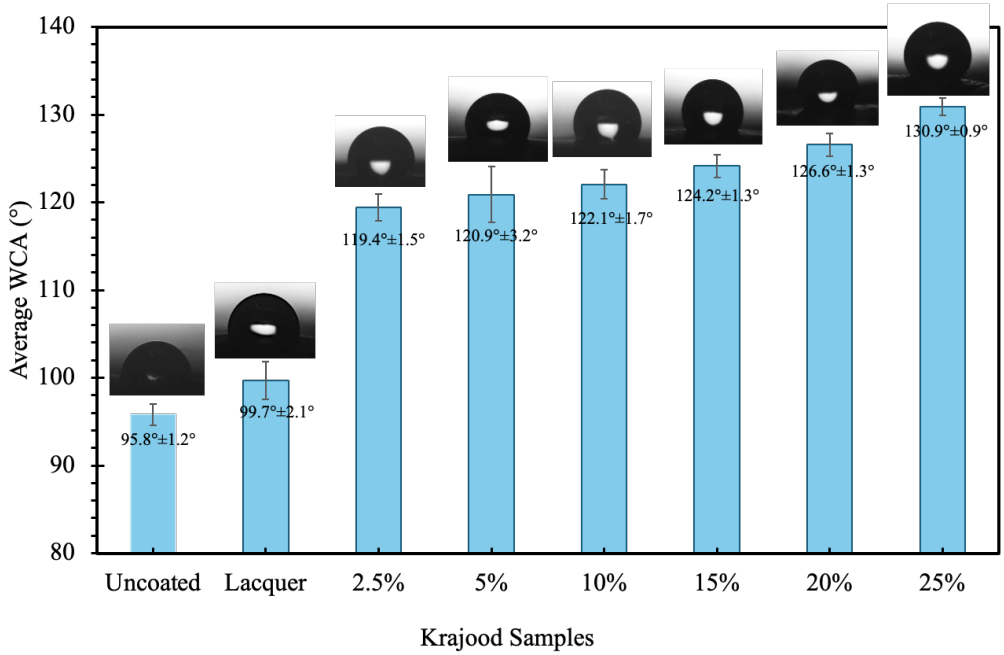

Figure 4 Water contact angle (WCA) measurements of Krajood samples: Uncoated, lacquer-coated, and coated with P(VDF-HFP) solutions at different concentrations (2.5, 5, 10, 15, 20 and 25%).

Mechanical properties

The mechanical properties of Krajood products, derived from 5 repeated tests for accuracy, highlight the significant impact of coatings on tensile strength, elongation at break, and stiffness, establishing P(VDF-HFP) as an optimal choice for coating applications. As shown in **Figure 5** and **Table 1**, uncoated samples exhibited the lowest tensile strength (86.41 ± 10.07 MPa), reflecting baseline structural limitations. Lacquer coatings moderately improved tensile strength to 99.77 ± 11.03 MPa due to the formation of a smooth, continuous surface layer that helped seal surface defects, reduce microcrack propagation, and improve fiber-to-fiber adhesion. This protective coating distributed mechanical stress more uniformly across the Krajood structure, resulting in enhanced resistance to tensile loading. P(VDF-HFP) coatings significantly enhanced the tensile strength of Krajood samples, with the highest value observed at 15.0% concentration (112.26 ± 10.18 MPa). This optimal performance is attributed to the formation of a uniform and sufficiently thick coating that promotes strong interfacial bonding between fibers, fills surface voids, and facilitates effective load transfer. At this concentration, the balance between the crystalline reinforcement from PVDF segments and the flexibility provided by HFP segments contributes to improved mechanical integrity without inducing brittleness. In contrast, lower concentrations may not provide adequate coverage or structural support, while higher concentrations (20.0 and 25.0%) resulted in reduced tensile strength (109.25 ± 10.69 and 95.55 ± 9.54 MPa, respectively), likely due to increased brittleness and non-uniform coatings caused by excessive polymer accumulation.

.

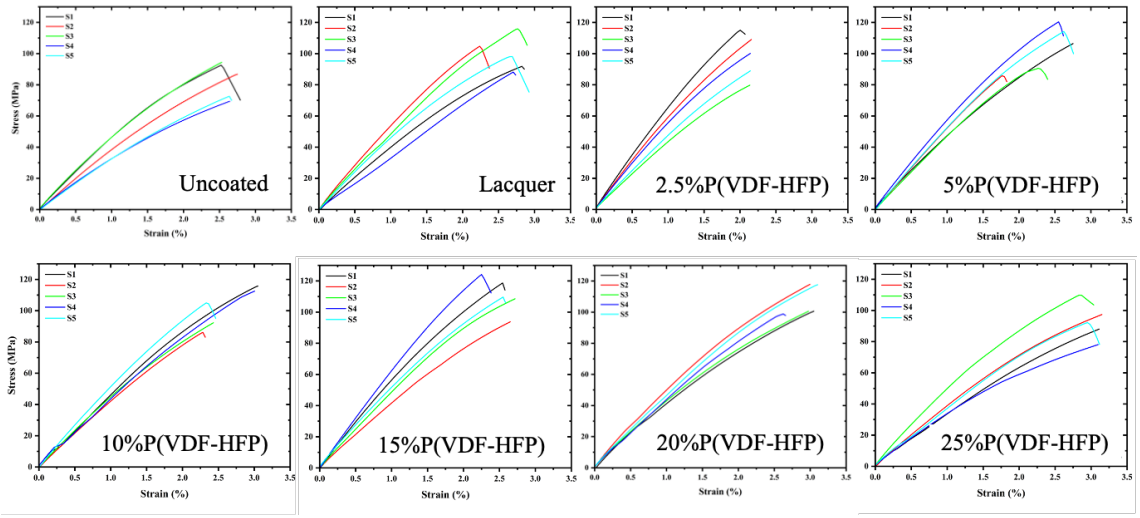

Figure 5 Stress-strain curves of Krajood samples: Uncoated, lacquer-coated, and coated with P(VDF-HFP) solutions at different concentrations (2.5, 5, 10, 15, 20 and 25 %).

Table 1 Mechanical properties results: tensile strength, elongation at break, and Young's modulus of Krajood products with different coatings, including uncoated sample, lacquer-coated sample, and samples coated with P(VDF-HFP) solution at varying concentrations.

Krajood products	Tensile strength (MPa)	Elongation at break (%)	Young's modulus (MPa)
Uncoated	86.41 ± 10.07	2.48 ± 0.40	40.75 ± 7.46
Lacquer	99.77 ± 11.03	2.30 ± 0.20	44.25 ± 7.79
2.5 % P(VDF-HFP)	102.31 ± 13.04	2.68 ± 0.24	46.32 ± 4.09

Krajood products	Tensile strength (MPa)	Elongation at break (%)	Young's modulus (MPa)
5.0 % P(VDF-HFP)	103.61 ± 14.94	2.76 ± 0.52	51.14 ± 4.18
10.0 % P(VDF-HFP)	104.58 ± 15.68	2.78 ± 0.25	54.10 ± 8.29
15.0 % P(VDF-HFP)	112.26 ± 10.18	2.88 ± 0.32	57.46 ± 5.54
20.0 % P(VDF-HFP)	109.25 ± 10.69	3.06 ± 0.23	47.00 ± 3.49
25.0 % P(VDF-HFP)	95.55 ± 9.54	3.32 ± 0.25	40.52 ± 7.57

Flexibility, as indicated by elongation at break, improved progressively with increasing P(VDF-HFP) concentration. The polymer's inherent flexibility, attributed to its amorphous HFP domains, allows it to deform under stress without breaking [29]. Uncoated samples displayed moderate elongation (2.48 ± 0.40%), while lacquer slightly reduced flexibility to 2.30 ± 0.20% due to its rigid nature. P(VDF-HFP) coatings enhanced ductility, reaching the highest elongation at break (3.32 ± 0.25%) at 25.0% concentration. Despite this peak in flexibility, excessive polymer concentrations compromised tensile strength and stiffness, underscoring the need for a balanced approach to achieve durability and flexibility in coated products.

Young's modulus, representing stiffness, also increased significantly with P(VDF-HFP) coatings. Uncoated samples exhibited the lowest modulus (40.75 ± 7.46 MPa), while lacquer slightly improved stiffness to 44.25 ± 7.79 MPa. P(VDF-HFP) coatings achieved maximum stiffness (57.46 ± 5.54 MPa) at 15.0% concentration, reflecting the dual contributions of its crystalline and amorphous domains. The crystalline VDF units provide structural support and mechanical strength, while the amorphous HFP domains enhance flexibility and facilitate electrolyte retention [30]. Beyond 15 %, the modulus declined (47.00 ± 3.49 MPa at 20.0% and 40.52 ± 7.57 MPa at 25.0%), likely due to softer regions and coating imperfections introduced by excessive polymer. These unique properties of P(VDF-HFP) allow it to improve adhesion and effectively fill gaps in Krajood fibers, resulting in superior coating performance. Thus, the 15.0% P(VDF-HFP) concentration offers the best combination of tensile strength, flexibility, and stiffness, leveraging the polymer's unique structural characteristics to enhance the durability and performance of Krajood products across various applications.

FTIR analysis

The FTIR analysis of Krajood samples clearly demonstrates the application of both lacquer and PVDF-HFP coatings, as evidenced by distinct spectral features unique to each treatment as represented in **Figure 6**. The uncoated Krajood samples primarily reflect their natural lignocellulosic composition, exhibiting key peaks associated with cellulose, hemicellulose, lignin, and possibly natural waxes [31]. A broad O–H stretching vibration around 3333 cm^{-1} indicates extensive hydrogen bonding among hydroxyl groups, typical of cellulose and lignin structures. The C–H stretching vibration at approximately 2920 cm^{-1} corresponds to the asymmetric and symmetric vibrations of methylene groups, indicating the presence of alkyl chains. Additionally, a peak near 1730 cm^{-1} is attributed to C=O stretching from carbonyl groups, likely from esters or aldehydes within hemicellulose and lignin. The presence of conjugated carbon-carbon bonds is suggested by the C=C stretching peak at around 1630 cm^{-1}, while the C–O stretching peak near 1031 cm^{-1} reflects the polysaccharide structure of cellulose and hemicellulose, consistent with typical lignocellulosic materials [32,33].

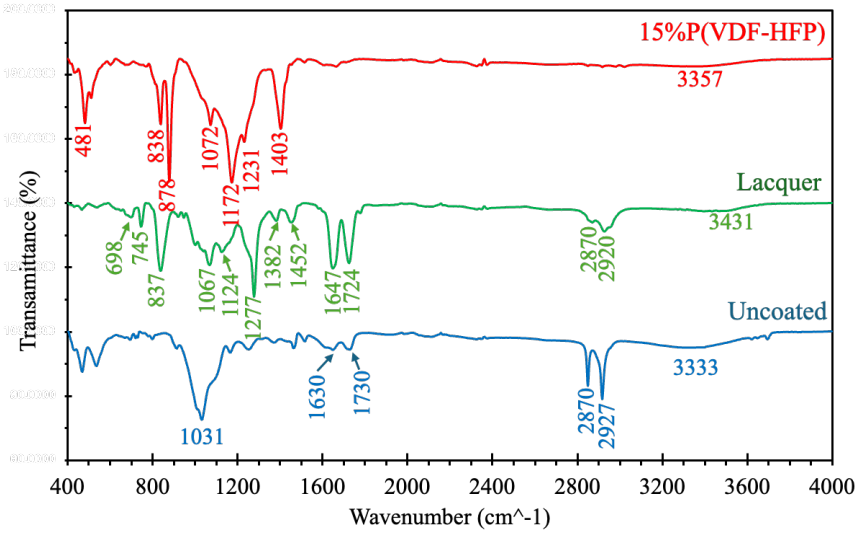

Figure 6 FTIR spectra of uncoated Krajood, lacquer-coated Krajood, and Krajood coated with 15.0% P(VDF-HFP) under nitrogen atmosphere.

Upon coating with lacquer, the FTIR spectrum of Krajood reveals several distinct peaks indicative of organic resin components, confirming the presence of the lacquer coating. A broad O–H stretching vibration, shifted and observed around 3431 cm^{-1}, suggests partial surface coverage of hydroxyl groups. Additionally, C–H stretching modes are evident from the absorption bands at 2920 and 2870 cm^{-1}, although all these peaks show reduced intensity compared to the uncoated sample, indicating surface modification and decreased availability of free –OH and $–CH_2$ groups due to the applied coating. A prominent carbonyl (C=O) stretching peak appears at approximately 1724 cm^{-1}, along with a C=C stretching band at 1647 cm^{-1}—both commonly associated with alkyd resins found in lacquer formulations. Additional bands at 1452 and 1382 cm^{-1} correspond to the bending and deformation vibrations of $–CH_2$ and $–CH_3$ groups. A strong absorption at 1277 cm^{-1} likely relates to C–O–C ester vibrations, further supporting the presence of alkyd-type components. Moreover, peaks at 1124 cm^{-1} are attributed to C–H bending as well as C–O and C–C stretching. Lastly, the absorption bands at 1067, 698, and 745 and 838 cm^{-1} are assigned to stretching and bending vibrations of the aromatic ring and aromatic C–H bonds, affirming the inclusion of aromatic structures characteristic of traditional lacquer compositions [34,35]. In contrast to the uncoated and lacquer-coated samples, the FTIR spectrum of Krajood coated with 15.0% P(VDF-HFP) reveals well-defined absorption bands characteristic of fluorinated polymers, confirming the successful application of the P(VDF-HFP) coating. Prominent peaks at approximately 1172 and 1072 cm^{-1} correspond to CF_2 antisymmetric stretching and CF_3 out-of-plane deformation, respectively, while a strong band at 1403 cm^{-1} is attributed to CH_2 scissoring. Additional peaks include 1231 cm^{-1} (CF wagging/deformation), 878 cm^{-1} (CH_2 rocking), 838 cm^{-1} (CH_2 rocking and CF_2 asymmetric stretching), and 767 cm^{-1} (CH_2 bending), all consistent with the characteristic region of P(VDF-HFP) [36,37]. These features, combined with the reduced intensity of the broad O–H stretching band around 3357 cm^{-1}, indicate effective masking of hydroxyl groups on the Krajood surface and confirm the presence of hexafluoropropylene units. This transformation enhances the surface's hydrophobicity and chemical resistance due to the fluorinated molecular structure of P(VDF-HFP), which provides low surface energy and chemical inertness, as well as the formation of micro/nano-scale surface textures during solvent evaporation. These textures trap air beneath water droplets, promoting the Cassie–Baxter wetting state, which minimizes liquid-solid contact and significantly increases water repellency while also improving resistance to chemical attack [38].

Thermal properties

Based on the detailed thermal analysis—including (a) TGA, (b) DTG, and (c) DTA curves presented in **Figure 7**—for uncoated Krajood, lacquer-coated Krajood, and Krajood coated with 15.0% P(VDF-HFP), significant differences are observed in thermal stability, degradation behavior, and energy response among the samples. A summary of the key thermal parameters is listed in **Table 2**. All 3 samples exhibit an initial mass loss below 120 °C due to the evaporation of physically absorbed water. Among them, the PVDF-HFP-coated sample shows the highest onset temperature (34.5 °C), compared to 30.3 °C for lacquer-coated and 28.7 °C for uncoated Krajood, indicating improved surface encapsulation and moisture resistance. This behavior is consistent with the nature of fluorinated polymers, which possess low surface energy and hydrophobicity, thereby limiting water permeability and thermal volatility [39]. During the main decomposition phase (~180 - 350 °C), the uncoated Krajood reveals prominent DTG peaks at 197.5, 268.2 and 334.8 °C, corresponding to the degradation of hemicellulose, cellulose, and lignin, respectively—core constituents of lignocellulosic biomass [40]. The lacquer-coated sample degrades slightly earlier (onset at 186.6 °C), attributed to the presence of thermally unstable ester and aromatic groups within the resin [41]. These compounds tend to decompose rapidly, releasing more energy during degradation (1399.68 mJ), as reflected in the DTA data. The increased energy output highlights the combined exothermic decomposition of both the fiber and lacquer components, possibly accelerating oxidative processes due to the presence of volatile organic compounds in the coating.

In contrast, the 15.0% P(VDF-HFP)-coated Krajood displays significantly improved thermal behavior, with a delayed decomposition onset at 241.9 °C and a smoother DTG profile, suggesting a more controlled degradation process. The principal decomposition peak at 272 °C and an additional high-temperature event at 484.8 °C are associated with the progressive breakdown of the fluorinated polymer. The P(VDF-HFP) copolymer, composed of vinylidene fluoride and hexafluoropropylene units, is known for its exceptional thermal and chemical resistance. Its degradation mechanism involves dehydrofluorination and cleavage of C–F and C–C bonds, contributing to the extended degradation range and thermal endurance of the coated fiber [42]. This is further supported by the lowest total energy release (1095.6 mJ) among the 3 samples, indicating that the fluoropolymer coating suppresses rapid thermal decomposition. Furthermore, the final degradation temperatures reinforce the superior protective effect of the P(VDF-HFP) coating. The uncoated sample degrades completely by 522.2 °C, while the lacquer-coated one ends at 494.9 °C. The P(VDF-HFP)-coated sample, although degrading by 492.9 °C, exhibits a more gradual and stable endset, maintaining some thermal integrity even beyond 480 °C. This not only improves fire resistance but also supports the structural and mechanical stability of the fiber in high-temperature environments. Thus, the incorporation of a 15.0% P(VDF-HFP) coating markedly enhances the thermal resistance and stability of Krajood fibers. Compared to both uncoated and lacquer-coated variants, the PVDF-HFP-coated Krajood demonstrates delayed degradation, reduced energy release, and sustained integrity at higher temperatures. The delayed degradation observed in P(VDF-HFP)-coated Krajood can be attributed to the polymer's strong carbon–fluorine bonds, which impart high thermal stability, as well as the formation of a protective barrier layer that limits heat transfer and oxidative exposure to the underlying natural fibers. These advantages are attributed to the coating's hydrophobicity, chemical inertness, and excellent thermal barrier properties, making it a promising material for extending the application of natural fibers in thermally demanding domains such as electronics, packaging, and flame-retardant composites.

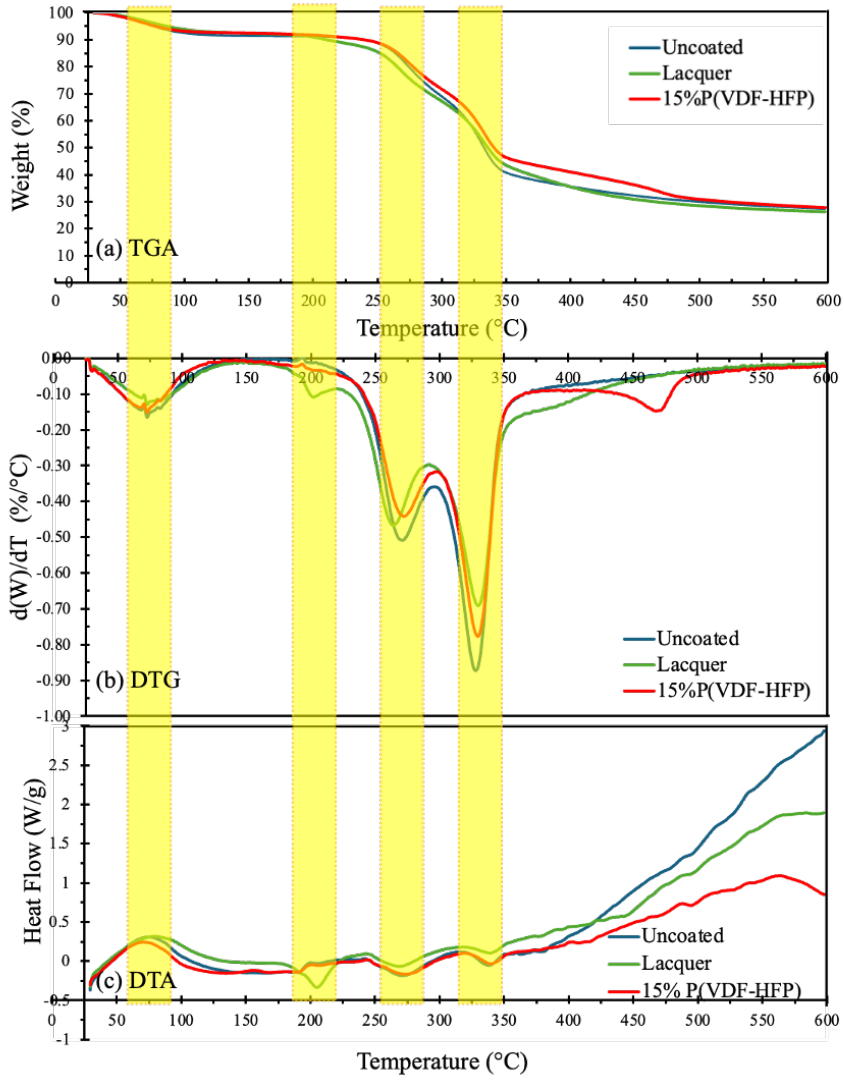

Figure 7 (a) TGA, (b) DTG, and (c) DTA thermograms of uncoated Krajood, lacquer-coated Krajood, and Krajood coated with 15 % P(VDF-HFP) under nitrogen atmosphere.

Table 2 Summary of key thermal properties derived from TGA, DTG, and DTA data for uncoated Krajood, lacquer-coated Krajood, and Krajood coated with 15.0% P(VDF-HFP).

Thermal Properties	Uncoated Krajood	Lacquer-Coated Krajood	15% P(VDF-HFP)-Coated Krajood
Initial Mass Loss Onset (°C)	28.73	30.28	34.5
Initial Mass Loss Peak (°C)	77.5	81.5	72.83
Initial Mass Loss Endset (°C)	114.22	125.7	107.85
Main Decomposition Onset (°C)	190.51	186.59	241.9
Main Decomposition Peak (°C)	197.5	202.17	272
Main Decomposition Endset (°C)	209.11	217.46	297.83
Final Degradation Peak (°C)	334.83	336.17	484.83

Thermal Properties	Uncoated Krajood	Lacquer-Coated Krajood	15% P(VDF-HFP)-Coated Krajood
Final Endset Temp (°C)	522.2	494.94	492.94
Highest Observed Peak (°C)	512.33	470.83	484.83
Total Energy Release (mJ)	1340.91	1399.68	1095.6
Normalized Energy (J/g)	149.7	149.7	122.46

SEM analysis of fungal inactivation

Figure 8 presents SEM micrographs of Krajood surfaces—uncoated, lacquer-coated, and coated with P(VDF-HFP) at concentrations ranging from 2.5 to 25.0%—captured at magnifications of 500×, 1,000×, 5,000×, and 10,000×. These images provide detailed insight into fungal colonization and the changes in surface morphology resulting from different coating treatments. The uncoated and lacquer-coated samples exhibited extensive fungal colonization, with numerous spherical spores adhering to the fiber surfaces. This suggests inadequate antifungal protection, likely due to the porous and hydrophilic characteristics of untreated Krajood and the limited barrier properties of the lacquer layer, consistent with the relatively low water contact angle (WCA) values of 95.81 and 99.70°, respectively [16]. The uncoated and lacquer-coated Krajood samples exhibited extensive fungal colonization due to their hydrophilic nature and lack of an effective antifungal barrier. The presence of cellulose and hemicellulose in natural fibers promotes moisture absorption, creating a favorable environment for fungal growth. While lacquer coating forms a surface film, it does not provide the same degree of hydrophobicity or structural protection as P(VDF-HFP), making it insufficient to inhibit fungal adhesion and proliferation over time.

In contrast, increasing concentrations of P(VDF-HFP) markedly reduced fungal adhesion. While 2.5 and 5.0% coatings still showed some fungal presence, coverage was sparse and irregular. From 10.0% onwards, surface morphology changed significantly, forming a denser and more uniform structure with prominent microporosity. This porous architecture became increasingly evident at concentrations of 15.0 to 25.0%. The formation of these pores, especially at concentrations above 10.0%, is attributed to the slower evaporation rate of the polymer solution during drying, which promotes phase separation and the development of micro- and nano-scale pores. The resulting surface roughness enhances water repellency by facilitating air entrapment, thereby minimizing contact between water droplets and the surface—corroborated by the increasing WCA values, reaching up to 130.9° at 25.0% [7,13,15]. Among all concentrations, the 15.0% P(VDF-HFP) coating delivered the most favorable balance of properties. SEM images revealed a well-distributed porous structure with minimal fungal presence. This coincided with the highest mechanical strength (112.26 MPa), Young's modulus (57.46 MPa), and a WCA of 124.2°, indicating excellent hydrophobicity and coating uniformity. Thermal analysis also confirmed enhanced thermal stability at this concentration, as shown by a delayed degradation onset (241.9 °C) and the lowest total energy release (1095.6 mJ), reflecting the material's effectiveness as a thermal barrier.

.

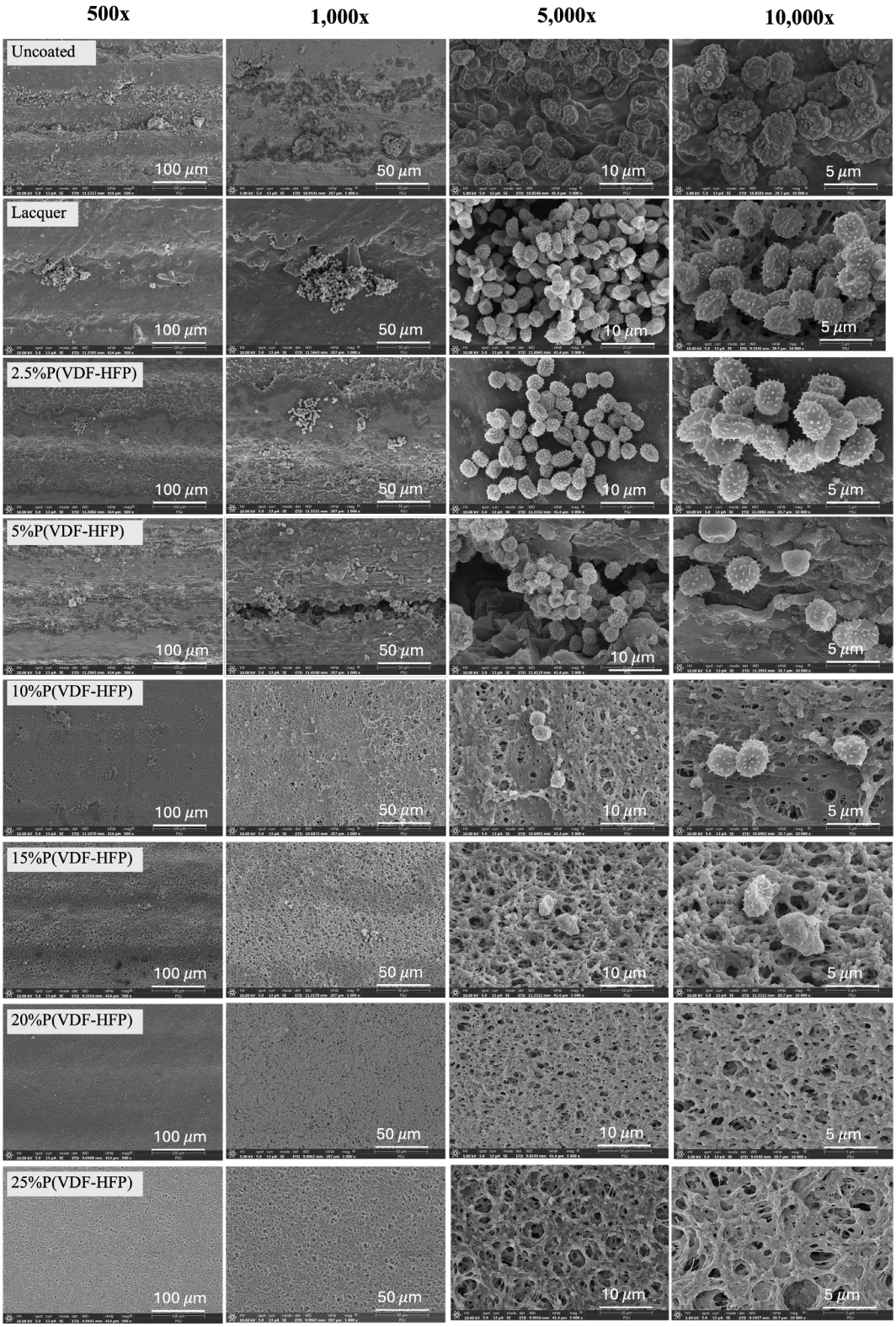

Figure 8 SEM images of Krajood products: uncoated, lacquer-coated, and coated with P(VDF-HFP) solutions at different concentrations (2.5, 5, 10, 15, 20 and 25%).

Although coatings at 20.0% and 25.0% P(VDF-HFP) concentrations continued to inhibit fungal growth effectively, they resulted in thicker, more opaque films and a slight decline in mechanical performance. This outcome can be attributed to the higher polymer content and increased viscosity of the coating solution, which caused slower spreading and reduced solvent evaporation during the drying process. As a result,

denser, layered films formed, with excessive polymer accumulation on the fiber surface—particularly in porous regions—leading to a more rigid and brittle structure. These characteristics contributed to diminished flexibility and strength, as reflected in the mechanical property data. Therefore, SEM analysis demonstrates that the 15.0% P(VDF-HFP) coating provides the most favorable balance of antifungal resistance, hydrophobicity, thermal durability, and mechanical integrity. The 15.0% P(VDF-HFP) coating delivered the most favorable balance of properties by achieving an optimal combination of coating uniformity, microporosity, and functional performance. At this concentration, the coating enhanced tensile strength and hydrophobicity, delayed thermal degradation, and effectively suppressed fungal growth, all while maintaining transparency and structural integrity. In contrast, higher concentrations introduced excess polymer accumulation, leading to increased brittleness, reduced mechanical performance, and less desirable optical properties. Its transparent appearance and suitable viscosity make it a highly effective and practical solution for extending the lifespan and functionality of Krajood products, especially in humid or microbial-prone environments.

Conclusions

This study successfully demonstrates the application of P(VDF-HFP) coatings as a multifunctional protective treatment for Krajood-based natural fiber products. Through systematic evaluation of samples coated with varying concentrations of P(VDF-HFP), it was found that the 15.0% concentration provided the best balance of properties—significantly improving hydrophobicity, mechanical strength, thermal stability, and resistance to fungal colonization. The enhanced water contact angle (124.2°) improved tensile strength (112.26 MPa), and delayed thermal degradation onset (241.9 °C) highlight the effectiveness of the coating in creating a durable and water-resistant barrier. SEM analysis further confirmed the reduction of fungal growth, attributed to the formation of microporous surface structures and the low surface energy of the fluorinated polymer. Compared to conventional lacquer coatings, the P(VDF-HFP) treatment offers a transparent, flexible, and environmentally stable alternative, making it highly suitable for extending the service life and maintaining the aesthetic quality of Krajood products in moisture-sensitive environments. This study builds upon and substantially expands earlier work by incorporating comprehensive characterization, statistical validation, and broader discussion on application potential. This work provides a foundation for future development of sustainable protective coatings for natural fibers in various industrial and craft applications.

Acknowledgments

This work was supported by Nakhon Si Thammarat Rajabhat University (NSTRU) and Thailand Science Research and Innovation (TSRI) through financial support from the Fundamental Fund 2567 (Grant No. NSTRU 005/2567). The authors would like to thank Nakhon Si Thammarat Rajabhat University for its instrumental role in supporting our research on the development of water-repellent and antifungal coatings for Krajood products. We also extend our appreciation to the Division of Physical Science (Physics), Faculty of Science, Prince of Songkla University, for their instrumental support, as well as to the faculty and staff at Nakhon Si Thammarat Rajabhat University for their continuous encouragement and resources throughout this study.

Declaration of generative AI in scientific writing

During the preparation of this work the authors used ChatGPT in order to check grammar. After using this tool, the authors reviewed and edited the content as needed and take full responsibility for the content of the publication

CRediT author statement

Sirikun Pethuan: Conceptualization; Formal analysis; Data curation; Investigation. **Nattavadee Tammachat:** Methodology. **Chaiporn Kaew-on:** Formal analysis. **Ratchaneewan Siri:** Methodology; Writing - Original draft. **Nikruesong Tohluebaji:** Writing - Original draft. **Phongpichit Channuie:** Writing - Original draft. **Jureeporn Yuennan:** Supervision; Conceptualization; Data curation; Formal analysis; Investigation; Methodology; Writing - Original draft preparation; Writing - Reviewing and Editing.

References

[1] K Chucheep, N Suwanpayak and N Phanchindawan. A study of the feasibility of using grey sedge residue to facilitate zero waste production. *Recycling* 2022; **7(3)**, 34.

[2] C Homkhiew, C Srivabut, S Rawangwong and W Boonchouytan. Performance of wood-plastic composites manufactured from post-consumer plastics and wood waste under coastal weathering in Thailand. *Fibers and Polymers* 2022; **23**, 2679-2693.

[3] CJF Rana, AL Quintos-Cortiguerra, AB Dorado and JJP Jimenez. Influence of lacquer sanding sealer treatment on the properties of bamboo waste particleboards for sustainable handicrafts. *Advances in Bamboo Science* 2025; **11**, 100158.

[4] Y Okahisa, C Narita and T Yoshimura. Resistance of wood coated with oriental lacquer (urushi) against damage caused by subterranean termite. *Journal of Wood Science* 2019; **65(1)**, 41.

[5] N Sgriccia, MC Hawley and M Misra. Characterization of natural fiber surfaces and natural fiber composites. *Composites Part A: Applied Science and Manufacturing* 2008; **39(10)**, 1632-1637.

[6] P Jin, C Huang, J Li, Y Shen and L Wang. Surface modification of poly(vinylidene fluoride) hollow fibre membranes for biogas purification in a gas–liquid membrane contactor system. *Royal Society Open Science* 2017; **4(11)**, 171321.

[7] X Wang, C Xiao, H Liu, Q Huang, J Hao and H Fu. Poly(vinylidene Fluoride-Hexafluoropropylene) porous membrane with controllable structure and applications in efficient oil/water separation. *Materials (Basel)* 2018; **11(3)**, 443.

[8] Y Liu, X Zhu, Y Chen, C Zhou, Z Chen, M Hao, X Hu and B Yang. Cross-electrospun PVDF/PVDF-HFP nanofibrous membrane with central combination design and its waterproof and moisture permeable composite fabric. *Textile Research Journal* 2023; **93(9-10)**, 2273-2289.

[9] J Yuennan, N Tohluebaji, C Putson, N Muensit and P Channuie. Enhanced electroactive β-phase and dielectric properties in P(VDF-HFP) composite flexible films through doping with three calcium chloride salts: CaCl, CaCl·2HO, and CaCl·6HO. *Polymers for Advanced Technologies* 2024; **35(6)**, e6437.

[10] H Wang, Z Liu, E Wang, R Yuan, D Gao, X Zhang and Y Zhu. A robust superhydrophobic PVDF composite coating with wear/corrosion-resistance properties. *Applied Surface Science* 2015; **332**, 518-524.

[11] J Knapczyk-Korczak, PK Szewczyk and U Stachewicz. The importance of nanofiber hydrophobicity for effective fog water collection. *RSC Advances* 2021; **11(18)**, 10866-10873.

[12] N Tohluebaji, R Siri, N Muensit, C Putson, P Channuie, P Porrawatkul and J Yuennan. Hydrophobic and optical properties of P(VDF-HFP) nanofiber filled with nickel (II) chloride hexahydrate for dye-sensitized solar cells application. *Trends in Sciences* 2024; **21(9)**, 8796.

[13] M Spasova, N Manolova, N Markova and I Rashkov. Superhydrophobic PVDF and PVDF-HFP nanofibrous mats with antibacterial and anti-biofouling properties. *Applied Surface Science* 2015; **363**, 363-371.

[14] DM Zhang, HD Wang, MC Huang,TT Fan, FQ Deng, CH Xue and XJ Guo. Fabrication of radiative cooling film with superhydrophobic self-cleaning property. *Surface Innovations* 2022; **11(5)**, 285-296.

[15] I Tournis, D Tsiourvas, Z Sideratou, LG Boutsika, A Papavasiliou, NK Boukos and AA Sapalidis. Superhydrophobic nanoparticle-coated PVDF-HFP membranes with enhanced flux, anti-fouling and anti-wetting performance for direct contact membrane distillation-based desalination. *Environmental Science: Water Research & Technology 2022*; **8(10)**, 2373-2380.

[16] J Žigon, UG Centa, M Remškar and M Humar. Application and characterization of a novel PVDF-HFP/PVP polymer composite with MoO(3) nanowires as a protective coating for wood. *Scientific Reports* 2023; **13(1)**, 3429.

[17] J Yuennan, C Kaew-on, A Khanklaeo, U Wanthong and C Sangpud. Development of water-repellent coating from P(VDF-HFP) polymer for krajood product substrate. *Journal of Science, Agriculture and Technology* 2024; **2(2)**, 22-32.

[18] G Concetto. Measurement of surface tension by the dripping from a needle. *Physics Education* 2006; **41(5)**, 440.

[19] NA Goy, Z Denis, M Lavaud, A Grolleau, N Dufour, A Deblais and U Delabre. Surface tension measurements with a smartphone. *The Physics Teacher* 2017; **55**, 498-499.

[20] M Nosonovsky and B Bhushan. Superhydrophobic surfaces and emerging applications: Non-adhesion, energy, green engineering. *Current Opinion in Colloid & Interface Science* 2009; **14(4)**, 270-280.

[21] K Manabe, M Saikawa, T Iwai and Y Norikane. Durable superhydrophobic surfaces on 3D-Printed structures inspired by beehive architecture. *Science and Technology of Advanced Materials* 2025; **26(1)**, 2481824.

[22] Y Pei and XC Zeng. Elastic properties of poly(vinyldene fluoride) (PVDF) crystals: A density functional theory study. *Journal of Applied Physics* 2011; **109(9)**, 093514.

[23] J Xu, Y Bai, M Wan, Y Liu, L Tao and X Wang. Antifungal paper based on a polyborneolacrylate coating. *Polymers* 2018; **10(4)**, 448.

[24] F Mokhtari, A Samadi, AO Rashed, X Li, JM Razal, L Kong, RJ Varley and S Zhao. Recent progress in electrospun polyvinylidene fluoride (PVDF)-based nanofibers for sustainable energy and environmental applications. *Progress in Materials Science* 2025; **148**, 101376.

[25] S Lee, JS Park and TR Lee. The wettability of fluoropolymer surfaces: Influence of surface dipoles. *Langmuir* 2008; **24(9)**, 4817-4826.

[26] N Rungruangkitkrai, P Phromphen, N Chartvivatpornchai, A Srisa, Y Laorenza, P Wongphan and N Harnkarnsujarit. Water repellent coating in textile, paper and bioplastic polymers: A comprehensive review. *Polymers* 2024; **16(19)**, 2790.

[27] G McHale, R Ledesma-Aguilar and C Neto. Cassie's law reformulated: composite surfaces from superspreading to superhydrophobic. *Langmuir* 2023; **39(31)**, 11028-11035.

[28] LK Sakti, GAN Sheha, CPSM Radhiyah, J Nugraha, DR Eddy, MD Permana, IP Maksum and Y Deawati. Cotton fabric coating by rGO and polymethylsiloxane layer with antibacterial, hydrophobic and photothermal properties. *Trends in Sciences* 2023; **20(11)**, 6813.

[29] A Tarhini and A Tehrani-Bagha. Graphene-based polymer composite films with enhanced mechanical properties and ultra-high in-plane thermal conductivity. *Composites Science and Technology* 2019; **184**, 107797.

[30] R Singh, S Janakiraman, A Agrawal, S Ghosh, A Venimadhav and K Biswas. An amorphous poly(vinylidene fluoride-co-hexafluoropropylene) based gel polymer electrolyte for magnesium ion battery. *Journal of Electroanalytical Chemistry* 2020; **858**, 113788.

[31] A Galletti, A D'Alessio, D Licursi, C Antonetti, G Valentini, A Galia and NND Nasso. Midinfrared FT-IR as a tool for monitoring herbaceous biomass composition and its conversion to furfural. *Journal of Spectroscopy* 2015; **2015**, 1-12.

[32] Z He, Y Liu, HJ Kim, H Tewolde and H Zhang. Fourier transform infrared spectral features of plant biomass components during cotton organ development and their biological implications. *Journal of Cotton Research* 2022; **5(1)**, 11.

[33] R Javier-Astete, J Jimenez-Davalos and G Zolla. Determination of hemicellulose, cellulose, holocellulose and lignin content using FTIR in Calycophyllum spruceanum (Benth.) K. Schum. and Guazuma crinita Lam. *PLoS One* 2021; **16(10)**, e0256559.

[34] A Heginbotham, M Schilling, H Khanjian and R Rivenc. A procedure for the efficient and simultaneous analysis of Asian and European lacquers in furniture of mixed origin. *In*: Proccedings of the International Council of Museums - Committee for Conservation, New Delhi, India. 2008.

[35] A Koochakzaei, AN Babaylou and BJ Bidgoli. Identification of coatings on persian lacquer papier mache penboxes by fourier transform infrared spectroscopy and luminescence imaging. *Heritage* 2021; **4(3)**, 1962-1969.

[36] C Kaew-on, J Yuennan, N Tohluebaji, P Channuie, S Ruangdit, R Samran, T Tochomphoo and R Siri. Enhanced hydrophobicity, thermal stability, and x-ray shielding efficiency of $BaSO_4$/P(VDF-HFP) nanocomposites for

advanced lead-free radiation protection. *Polymers* 2025; **17(6)**, 723.

[37] L Li, H Li, Y Wang, S Zheng, Y Zou and Z Ma. Poly(vinylidenefluoride-hexafluoropropylene)/cellulose/carboxylic TiO_2 composite separator with high temperature resistance for lithium-ion batteries. *Ionics* 2020; **26(9)**, 4489-4497.

[38] BJ Deka, EJ Lee, J Guo, J Kharraz and AK An. Electrospun nanofiber membranes incorporating PDMS-aerogel superhydrophobic coating with enhanced flux and improved antiwettability in membrane distillation. *Environmental Science & Technology* 2019; **53(9)**, 4948-4958.

[39] S Rasouli, N Rezaei, H Hamedi, S Zendehboudi and X Duan. Superhydrophobic and superoleophilic membranes for oil-water separation application: A comprehensive review. *Materials & Design* 2021; **204**, 109599.

[40] M Goliszek, B Podkościelna, T Klepka and O Sevastyanova. Preparation, thermal, and mechanical characterization of uv-cured polymer biocomposites with lignin. *Polymers* 2020; **12(5)**, 1159.

[41] Q Xiao, Y Cao, H Tan, Q Feng, X Gu, J Lyu, H Xiao, M Chen and Y Chen. Preparation and properties of chinese lacquer modified by methylolureas. *Journal of Renewable Materials* 2023; **11(2)**, 1003-1016.

[42] P Shabeeba, J kavil, P Shameela, P Sreya and N Aparna. Room temperature ionic liquids encapsulated PVDF-HFP gel electrolytes for flexible supercapacitors. *Next Materials* 2025; **6**, 100330.